Colonic Dilation and Altered *Ex Vivo* Gastrointestinal Motility in the Neuroligin-3 Knockout Mouse

Anita J. L. Leembruggen, Gayathri K. Balasuriya, Jinghong Zhang, Shana Schokman, Kristy Swiderski, Joel C. Bornstein, Jess Nithianantharajah, and Elisa L. Hill-Yardin

Gastrointestinal (GI) dysfunction is commonly reported by people diagnosed with autism spectrum disorder (ASD; autism) but the cause is unknown. Mutations in genes encoding synaptic proteins including Neuroligin-3 are associated with autism. Mice lacking Neuroligin-3 ($Nlgn3^{-/-}$) have altered brain function, but whether the enteric nervous system (ENS) is altered remains unknown. We assessed for changes in GI structure and function in $Nlgn3^{-/-}$ mice. We found no significant morphological differences in villus height or crypt depth in the jejunum or colon between wildtype (WT) and $Nlgn3^{-/-}$ mice. To determine whether deletion of Nlgn3 affects enteric neurons, we stained for neural markers in the myenteric plexus. $Nlgn3^{-/-}$ mice had similar numbers of neurons expressing the pan-neuronal marker Hu in the jejunum, proximal mid, and distal colon regions. We also found no differences in the number of neuronal nitric oxide synthase (nNOS+) or calretinin (CalR+) motor neurons and interneurons between WT and $Nlgn3^{-/-}$ mice. We used *ex vivo* video imaging analysis to assess colonic motility under baseline conditions and observed faster colonic migrating motor complexes (CMMCs) and an increased colonic diameter in $Nlgn3^{-/-}$ mice, although CMMC frequency was unchanged. At baseline, CMMCs were faster in $Nlgn3^{-/-}$ mice compared to WT. Although the numbers of neuronal subsets are conserved in $Nlgn3^{-/-}$ mice, these findings suggest that Neuroligin-3 modulates inhibitory neural pathways in the ENS and may contribute to mechanisms underlying GI disorders in autism. ***Autism Res*** *2020, 13: 691–701.* © 2019 The Authors. *Autism Research published by International Society for Autism Research* published by Wiley Periodicals, Inc.

Lay Summary: People with autism commonly experience gut problems. Many gene mutations associated with autism affect neuronal activity. We studied mice in which the autism-associated *Neuroligin-3* gene is deleted to determine whether this impacts gut neuronal numbers or motility. We found that although mutant mice had similar gut structure and numbers of neurons in all gut regions examined, they had distended colons and faster colonic muscle contractions. Further work is needed to understand how Neuroligin-3 affects neuron connectivity in the gastrointestinal tract.

Keywords: autism; gastrointestinal symptoms; gut motility; Neuroligin-3; mouse models; immunofluorescence

Introduction

Autism spectrum disorder (ASD; autism) is a highly prevalent neurodevelopmental disorder with current figures suggesting that 1 in 59 children are affected in the United States [Baio et al., 2018]. ASD is diagnosed based on impaired social interaction and communication, and restrictive and repetitive behaviors [APA DSM-5, 2013]. The prevalence of gastrointestinal (GI) disorders (e.g., acute constipation, diarrhea, and abdominal pain) is increased in patients with autism compared to the general population [Valicenti-McDermott et al., 2006]. Children diagnosed with autism are twice as likely to be prescribed medication for GI disorders and four times more likely to be hospitalized with GI disorders compared to neurotypical children [Croen, Najjar, Ray, Lotspeich, & Bernal, 2006; McElhanon, Mccracken, Karpen, & Sharp, 2014; Valicenti-McDermott et al., 2006]. A meta-analysis of 84 studies of GI dysfunction in autism patients identified a median prevalence of 22.2% for constipation, 13% for diarrhea, and 46.8% for any GI symptom [Holingue et al., 2018]. Additional studies have identified that 60–74% of children patients with autism experience inflammation of the small or large intestine [Horvath, Papadimitriou, Rabsztyn, Drachenberg, & Tildon, 1999; Krigsman et al., 2010].

Autism has a strong genetic component, with monozygotic twins more likely to be diagnosed with autism compared to dizygotic twins [Bailey et al., 1995; Folstein & Rosen-Sheidley, 2001; Steffenburg et al., 1989]. Additionally,

From the Department of Physiology, University of Melbourne, Melbourne, Victoria, Australia (A.J.L.L., J.Z., J.C.B., E.L.H.-Y.); School of Health and Biomedical Sciences, RMIT University, Bundoora, Victoria, Australia (G.K.B., S.S., E.L.H.-Y.); Centre for Muscle Research, Department of Physiology, University of Melbourne, Melbourne, Victoria, Australia (K.S.); Florey Institute of Neuroscience and Mental Health, Melbourne, Victoria, Australia (J.N.)

Anita J. L. Leembruggen and Gayathri K. Balasuriya are co-first authors.

Received February 10, 2019; accepted for publication April 1, 2019

Address for correspondence and reprints: Elisa L. Hill-Yardin, School of Health and Biomedical Sciences, RMIT University, Bundoora, VIC, Australia. E-mail: elisa.hill@rmit.edu.au

Published online 19 April 2019 in Wiley Online Library (wileyonlinelibrary.com)
DOI: 10.1002/aur.2109

in 10–20% of autism cases, rare genetic mutations that are thought to underlie the core symptoms are expressed [Betancur, 2011; Geschwind, 2011; Voineagu et al., 2011]. Of over 1,000 genes implicated in the development of autism [Basu, Kollu, & Banerjee-Basu, 2009], many are involved in nervous system development and synaptic transmission [Cristino et al., 2014]. Multiple mutations in proteins involved in neuronal communication are associated with autism, including in Neuroligin-3 (*Nlgn3*) and associated synaptic proteins [Alarcón et al., 2008; Arking et al., 2008; Bakkaloglu et al., 2008; Bourgeron, 2015; Comoletti et al., 2004; Durand et al., 2007; Feyder et al., 2010; Jamain et al., 2003; Moessner et al., 2007; Phelan et al., 2001].

There has been little investigation into the effect of autism-associated mutations on the enteric nervous system (ENS), the intrinsic nervous system of the gut. The ENS comprises the submucosal plexus, which primarily regulates the secretion of water and electrolytes into the gut lumen, and the myenteric plexus (MP), which regulates the movement of food within the gut [reviewed in Furness, 2012].

Approximately 20–40% of neurons in the mouse MP are immunoreactive (IR) for neuronal nitric oxide synthase [nNOS; Sang & Young, 1996]. Nitric oxide (NO) is an inhibitory neurotransmitter in the ENS and is expressed in inhibitory motor neurons, as well as a subset of descending (anally projecting) interneurons [Furness, 2000; Brookes, 1993; Brookes, 2001]. Other myenteric neurons express the calcium binding protein Calretinin (CalR) including ascending (orally projecting) interneurons, and intrinsic sensory neurons. These neurons receive and relay information regarding distention, pH levels, and solute concentrations in the gut via signaling from enterochromaffin cells located in the gut epithelium [Furness, 2006; Surawicz, 2010] to motor and interneurons to coordinate gut function [Bertrand, Kunze, Bornstein, Furness, & Smith, 1997].

Genes encoding the neuroligin (NLGN) family of cell adhesion molecules are implicated in autism [Jamain et al., 2003], synaptogenesis [Shen, Huo, Zhao, Wang, & Zhong, 2015], and the maintenance of synaptic structural integrity via binding to various postsynaptic proteins such as PSD-95 [Sudhof, 2008]. Although mutations in *Nlgn3* are rare, neuroligins are part of postsynaptic signaling complex within which many mutations cause autism [Betancur, Sakurai, & Buxbaum, 2009; reviewed in Bourgeron, 2009]. It is therefore of interest to characterize changes in GI structure and function caused by mutations in *Nlgn3*. A deletion of the *Nlgn3* gene was observed in a male diagnosed with ASD [Levy et al., 2011] and in another case with pervasive developmental disorder not otherwise specified [Sanders et al., 2011]. A missense mutation in *Nlgn3* causing the substitution of a conserved arginine for a cysteine residue at position 451 within the NLGN3 protein was identified in two brothers diagnosed with ASD [Jamain et al., 2003].

Mice null for Neuroligin-3 ($Nlgn3^{-/-}$) have reduced vocalizations and social interaction [Jaramillo, Liu, Pettersen, Birnbaum, & Powell, 2014; Radyushkin et al., 2009], congruent with impaired social communication in autism. $Nlgn3^{-/-}$ mice also display altered neurophysiology in the brain. Specifically, $Nlgn3^{-/-}$ mice display a decreased frequency of miniature excitatory postsynaptic currents and an increased frequency of miniature inhibitory postsynaptic currents in the hippocampus [Etherton et al., 2011]. $Nlgn3^{-/-}$ mice also have increased GABAergic neurotransmission at cholecystokinin-immunoreactive basket cell synapses [Földy, Malenka, & Südhof, 2013], and impaired tonic cannabinoid signaling [Földy et al., 2013], further demonstrating altered synaptic function.

Here, we aimed to determine whether deletion of the Neuroligin-3 synaptic protein impacts GI structure or function by assessing for regional structural changes at the histological and cellular levels as well as examining *ex vivo* colonic motility.

Material and Methods

Animals

$Nlgn3^{-/-}$ mice were originally generated via homologous recombination of embryonic stem cells to induce deletion of at least 380 base pairs of 5′ coding of the *Nlgn3* gene [Varoqueaux et al., 2006] and subsequently bred onto C57Bl/6NCrl mice for more than 10 generations [Radyushkin et al., 2009]. $Nlgn3^{-/-}$ mice and their respective WT littermate matched controls were generated by mating heterozygous females with WT males. Genotypes of male 12-week-old mice were verified by polymerase chain reaction and confirmed with Western blots of brain homogenates from homozygous $Nlgn3^{-/-}$ mice demonstrating a lack of full length NL3 or truncated variants in the $Nlgn3^{-/-}$ mice. Mice processed for immunofluorescent staining were anesthetized with 0.05 mL pentobarbitate before transcardial perfusion with 4% paraformaldehyde (PFA) at a rate of 10 mL/min for 3 min. Animals used for video imaging experiments were killed via cervical dislocation, as approved by the Florey Institute Animal Ethics Committee (Ethics ID: 14-095).

Histology

To investigate the effects of *Nlgn3* deletion on GI structure, transverse sections of the proximal jejunum and proximal colon were stained with hematoxylin and eosin. Sections of proximal jejunum and proximal colon from WT and $Nlgn3^{-/-}$ mice were dissected and placed in individual 1.5 mL Eppendorf tubes filled with 4% PFA to postfix at 4°C overnight. The tissue was rinsed three times in phosphate buffered saline (PBS) for 10 min and incubated in a 30% sucrose solution overnight at 4°C. The tissue sections were placed in optimal cutting temperature medium (Tissue Tek, Elkhart IN) and immediately snap frozen in iso-pentane cooled with liquid nitrogen. Frozen tissue preparations were cross-sectioned at 10-μm thickness using a cryostat (Microm HM 525, Fronine Laboratory

Supplies, Riverstone, NSW, Australia). Tissue sections were then mounted onto positively charged slides (SuperFrostPlus, Menzel-Glaser, Braunschweig, Germany) and left at room temperature (RT) (in a fume hood) for 1 hr prior to staining. Following staining, coverslips were secured to the slides using DPX mounting medium (Merck, Darmstadt, Germany), and left to dry overnight.

Histological Parameters

Brightfield images of stained sections were obtained using a Zeiss Axio Imager D1 Microscope (Gladesville, NSW, Australia), and analyzed for villus height and crypt depth using ImageJ/FIJI software (Version 1.49d, NIH). Only villi with the full lacteal visible were measured for villus height (the length between tip of the villus and the villus/crypt junction), with a minimum of 10 villi per animal measured in WT ($n = 5$) and Nlgn3$^{-/-}$ ($n = 5$) mice from approximately 10 tissue sections. Crypt depth was measured as the length between the base of the crypt and the villus/crypt junction. Measurements were obtained from both the proximal jejunum and proximal colon. At least 10 crypts per animal were measured in WT and Nlgn3$^{-/-}$ mice.

Immunofluorescence

To assess for changes in neuronal subpopulations, myenteric preparations were labeled for nNOS and CalR that together, label approximately 70–75% of myenteric neurons [Sang & Young, 1996]. The proximal jejunum and entire colon were dissected, opened along the mesenteric border and pinned in a petri dish lined with silicone elastomer (Sylgard 184, Dow Corning), before being postfixed overnight in 4% PFA at 4°C. Fixed tissue was rinsed three times at 10-min intervals in PBS (pH = 7.2). The mucosa, submucous plexus, and circular muscle were peeled away from the underlying MP. Longitudinal muscle myenteric plexus preparations were permeabilized in CASBLOCK +0.1% Triton for 30 min at RT, prior to incubation in primary antisera (Table 1) at 4°C for 24–48 hr. Each tissue preparation was rinsed in PBS three times at 10 min intervals before incubation with secondary antibodies (Table 2) for 2 hr at RT. Following an additional round of PBS rinses, the tissue preparations were mounted onto glass microscope slides in DAKO fluorescence mounting medium (DAKO, Carpenteria, CA) and secured with a glass coverslip. An Axio Imager2 fluorescence microscope was used to image 4–5 randomly selected areas per whole mount preparation. All images were exported as .tiff files to preserve resolution and were adjusted for brightness and contrast using ImageJ/FIJI.

Cell Counts

To count neurons, the "Cell Counter" plugin on ImageJ/FIJI (Version 1.49d, NIH) was used. Neurons IR for Hu were manually counted in a single field of view (2,752 pixels × 2,208 pixels; 625 × 501 μm^2, total area of 0.3 mm^2). All whole neurons and neurons intersecting the bottom and left borders of the image were counted; however, neurons intersecting the top and right borders of the image were not included. Counts were performed by two assessors blind to the genotype (WT or Nlgn3$^{-/-}$) of the tissue preparations. Cell count data, which was obtained as the number of neurons per 0.3 mm^2, were converted to the number of neurons per mm^2.

Table 1. Primary Polyclonal Antisera Used for Immunohistochemistry

Primary antibody	Host species	Concentration	Source
Hu	Human	1:5,000	Kind gift from Dr. V. Lennon
nNOS	Sheep	1:1,000	Kind gift from Dr. P. Emson
Calretinin	Goat	1:1,000	Swant (CG1)

Immunoprecipitation and Western Immunoblotting to Confirm Neuroligin-3 Expression in Colon

Snap frozen brain, proximal colon, and distal colon tissue from WT and Nlgn3$^{-/-}$ mice were homogenized in lysis buffer [1% v/v Triton X-100, 50 mM Tris–HCl pH 7.5, 150 mM NaCl, 1 mM EDTA, 2 mM Na_3VO_4, 50 mM NaF, and complete protease inhibitor cocktail (Roche Applied Science)]. Lysates were cleared by centrifugation at 20,000*g* for 10 min at 4°C and incubated 2 hr at 4°C on rotating wheel with 50 μL protein A sepharose 4B (PAS; Thermo Fisher Scientific; Waltham, MA). Cleared lysates (100 μg for brain, 2.5 mg for colon) were subject to immunoprecipitation with an antibody directed to Neuroligin-3 (3 μg per sample, Rabbit-α-Neuroligin 3; Synaptic systems Cat #129113) at 4°C overnight (o/n) and immune complexes were captured the next day with PAS for 2 hr at 4°C. Beads were washed three times with high salt lysis buffer [1% v/v Triton X-100, 50 mM Tris–HCl pH 7.5, 300 mM NaCl, 1 mM EDTA, 2 mM Na_3VO_4, 50 mM NaF, and complete protease inhibitor cocktail (Roche Applied Science)] and immunocaptured proteins were eluted by incubation for 5 min at 95°C. Eluted proteins were separated by SDS-PAGE alongside a molecular weight marker (Precision Plus Protein™ all blue prestained protein standard, Bio-Rad Laboratories, Hercules, CA) on a 4–12% gradient mini-PROTEAN TGX pre-cast gel (Bio-Rad Laboratories), and transferred to polyvinylidene difluoride (PVDF) membrane by semi-dry transfer on a Trans-blot turbo (Bio-Rad Laboratories). Membranes were blocked in 5% bovine serum albumin (BSA)/tris-buffered saline with 0.1%

Table 2. Secondary Polyclonal Antisera Used for Immunohistochemistry

Secondary antibody	Host species	Concentration	Source
Human Alexa 594	Donkey	1:5,000	Molecular probes (A11001)
Human Alexa 647	Donkey	1:500	Jackson (709-605-149)
Sheep Alexa 488	Donkey	1:400	Molecular probes (A11015)

tween-20 (TBST) for 1 hr at RT and incubated o/n at 4°C with the antibody directed to Neuroligin-3 (1:1,000 in 5% BSA/TBST). Membranes were washed 3× 5 min with TBST, incubated 1 hr at RT with horseradish peroxidase-conjugated donkey antirabbit immunoglobulin (1:5,000 in 5% BSA/TBST; GE Healthcare Life Sciences; Marlborough, MA), washed 4× 10 min in TBST and developed by enhanced chemiluminescence (ECL Prime; GE Healthcare Life Sciences) on a ChemiDoc MP Imaging System (Bio-Rad Laboratories).

Video Imaging

Colonic motility was recorded ex vivo using a Logitech camera (QuickCam Pro 4000; I-Tech, Ultimo, NSW, Australia) mounted directly above an organ bath as previously described [Balasuriya, Hill-Yardin, Gershon, & Bornstein, 2016; Swaminathan et al., 2016]. Experiments consisted of control, drug, and drug washout recordings (each consisting of four segments of 15 min recordings). The nNOS inhibitor Nω-nitro-L-arginine (NOLA) was applied to the organ bath and resulting contractions were compared between Nlgn3$^{-/-}$ mice and their WT littermates. Using the in-house software Scribble 2.0 and the Matlab (2013b) plugin Analyse 2.0, recorded videos were converted to spatiotemporal maps reflecting the diameter of the colon along the length of the tissue (*y*-axis) as a function of time (*x*-axis). A color bar indicated luminal diameter, where pixels with cool colors (e.g., blue-green) indicated dilated tissue, whereas pixels with warmer colors (e.g., yellow-red) indicated a constricted colon. CMMCs originating at the oral end of the colon and propagating more than half of the length of the tissue were included for analysis. Recordings were analyzed for the number of CMMCs, CMMC speed, and resting colonic diameter, as described by Swaminathan et al. [2016] and Balasuriya et al. [2016]. Briefly, CMMC frequency was manually counted from spatiotemporal maps and resting gut diameter (the diameter of the relaxed colon in between CMMCs) was derived from a data point in spatiotemporal maps at two-thirds of the colonic length from the oral end.

Statistical Analysis

Statistical analysis was performed using Graphpad Prism (Version 7.05, CA). Villus height, crypt depth, and cell count data were analyzed using two-tailed, unpaired *t* tests and one-way ANOVA. CMMC speed and resting gut diameter data were analyzed using a Student's *t* test with Bonferroni correction for multiple comparisons. CMMC numbers were analyzed using a Mann–Whitney test. Data are presented as mean ± SEM.

Results

To establish whether deletion of Neuroligin-3 affects gut structure and function, we assessed colonic crypt depth, jejunal crypt depth and villus height, neuronal subpopulations, and colonic motility in the GI tract of WT and Nlgn3$^{-/-}$ mice.

There were no obvious differences in the major morphological features of the jejunum between WT and Nlgn3$^{-/-}$ mice. Both WT and Nlgn3$^{-/-}$ mice had typical jejunal morphology, with no visible structural damage evident at the villus tips (Fig. 1A). WT and Nlgn3$^{-/-}$ mouse colon tissue structure was also similar (Fig. 1B). Additionally, there was no difference in villus height between WT and Nlgn3$^{-/-}$ mice (WT: 244 ± 11 μm, $n = 5$; Nlgn3$^{-/-}$: 249 ± 8 μm, $n = 5$, $P = 0.73$ Fig. 1C). Crypt depth in the jejunum (WT: 37 ± 1 μm, $n = 5$; Nlgn3$^{-/-}$: 39 ± 1 μm, $n = 5$, $P = 0.33$) and colon (WT: 47 ± 3 μm, $n = 5$; Nlgn3$^{-/-}$: 42 ± 2 μm, $n = 5$, $P = 0.22$) were also unchanged in Nlgn3$^{-/-}$ mice (Fig. 1D) suggesting that the absence of Neuroligin-3 produces no overt changes in mucosal structure in these regions. There were no overt signs of GI abnormality in mice lacking *Nlgn3* upon removing the colon from the animal.

To determine if neuronal number is altered in Nlgn3$^{-/-}$ mice, we labeled myenteric neurons for the pan-neuronal marker, Hu. We observed a significant effect of gut region ($P < 0.0001$ (gut region), two-way ANOVA) whereby the highest numbers of neurons were found in the proximal colon, followed by the mid and distal colon, with the lowest numbers of neurons present in the proximal jejunum. However, there was no genotype difference in the total number of neurons in any region (Fig. 2A–C, $P = 0.44$ (genotype, two-way ANOVA)). The total number or Hu + neurons per mm^2 in the proximal jejunum (WT: 228 ± 8, $n = 5$; Nlgn3$^{-/-}$: 238 ± 22, $n = 5$), proximal colon (WT: 723 ± 104, $n = 5$; Nlgn3$^{-/-}$: 638 ± 35, $n = 5$), mid colon (WT: 597 ± 34, $n = 5$; Nlgn3$^{-/-}$: 721 ± 30, $n = 9$), or distal colon (WT: 390 ± 26, $n = 8$; Nlgn3$^{-/-}$: 432 ± 30, $n = 9$) were similar in WT and Nlgn3$^{-/-}$ mice.

We also investigated whether the number of nNOS+ neurons and CalR+ neurons were altered in Nlgn3$^{-/-}$ and WT mice. As for the total number of neurons, the number of nNOS+ neurons per mm^2 was similar for both genotypes ($P = 0.09$, two-way ANOVA) and showed a significant difference between regions, with the lowest numbers of nNOS+ neurons in the proximal jejunum ($P < 0.0001$, two-way ANOVA, Fig. 2A, D). NOS+ neuronal numbers in the proximal jejunum of Nlgn3$^{-/-}$ mice were unchanged compared to WT (WT: 56 ± 2, $n = 5$; Nlgn3$^{-/-}$: 67 ± 5, $n = 5$). Similarly, there was no difference in the number of NOS+ neurons in the proximal colon (WT: 161 ± 24, $n = 5$; Nlgn3$^{-/-}$: 189 ± 21, $n = 5$), mid colon (WT: 144 ± 33, $n = 5$; Nlgn3$^{-/-}$: 180 ± 30, $n = 5$), or distal colon (WT: 39 ± 10, $n = 5$; Nlgn3$^{-/-}$: 178 ± 19, $n = 5$). The number of CalR+ neurons was also similar in the proximal jejunum (WT: 29 ± 1.7, $n = 5$; Nlgn3$^{-/-}$: 28 ± 3, $n = 5$), proximal colon (WT: 65 ± 11, $n = 4$; Nlgn3$^{-/-}$: 46 ± 2, $n = 3$), mid colon (WT: 131 ± 22, $n = 5$; Nlgn3$^{-/-}$: 158 ± 19, $n = 8$), and distal colon (WT: 39 ± 10, $n = 6$; Nlgn3$^{-/-}$: 40 ± 3, $n = 7$) of WT and Nlgn3$^{-/-}$ mice ($P = 0.62$, two-way ANOVA; Fig. 2B, E). There

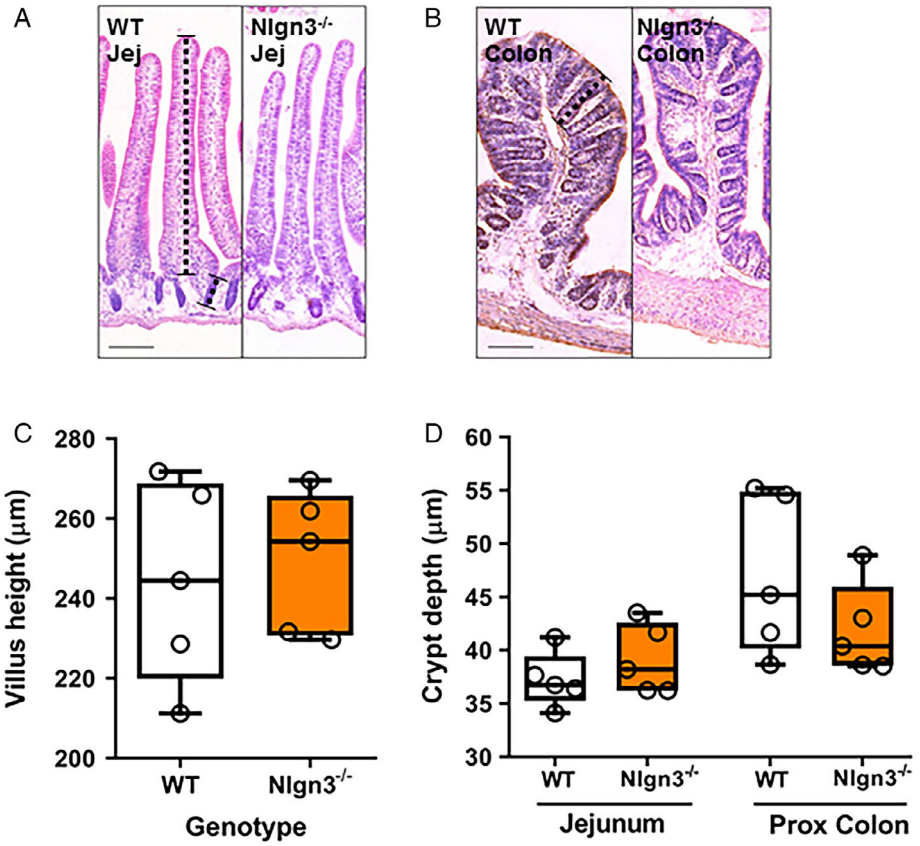

Figure 1. Comparison of GI morphology in WT and Nlgn3$^{-/-}$ mice. Sections of Nlgn3$^{-/-}$ and WT jejunum (**A**), and colon (**B**) stained with Hematoxylin and Eosin. There was no difference in villus height in the jejunum (**C**) between WT and Nlgn3$^{-/-}$ mice (n = 5 in each group), or crypt depth in the jejunum or colon (**D**) in either genotype (n = 5 in each group). Scale bars = 50 μm. Statistics: Student's t test. Villus height and crypt depth were measured as indicated by the broken lines in the left panel of A.

was a significant difference in the number of CalR+ neurons observed between the gut regions, with the lowest numbers found in the proximal jejunum (P = 0.006, two-way ANOVA). These findings indicate that the deletion of Nlgn3 does not affect the total number of myenteric neurons or the numbers of nNOS or CalR IR neurons in the mouse proximal jejunum or colon MP.

We then assessed for potential alterations to proportions of motor neurons or interneurons in Nlgn3$^{-/-}$ mice by labeling MP preparations for nNOS and CalR and calculating the mean proportion of each of these markers as a percentage of the total neuronal population (IR for Hu). Although we observed a significant difference in the proportion of nNOS+ neurons between gut regions in both genotypes, whereby the distal colon had the highest proportion of nNOS+ neurons (P = 0.001, two-way ANOVA), there was no difference in the proportion of nNOS+ neurons between WT and Nlgn3$^{-/-}$ mice (Fig. 2, P = 0.34, two-way ANOVA). We observed no significant difference in the proportion of nNOS+ neurons between WT and Nlgn3$^{-/-}$ mice in the proximal jejunum (WT: 26 ± 1%, n = 5; Nlgn3$^{-/-}$: 27 ± 0.8%, n = 5), proximal colon (WT: 26 ± 2%, n = 5; Nlgn3$^{-/-}$: 30 ± 3%, n = 5), mid colon (WT: 25 ± 5%, n = 5; Nlgn3$^{-/-}$: 29 ± 3%, n = 5), or distal colon (WT: 40 ± 2.5%, n = 5; Nlgn3$^{-/-}$: 40 ± 7%, n = 5). Additionally, similar proportions of CalR+ neurons were present in the proximal jejunum (WT: 40 ± 2%, n = 5; Nlgn3$^{-/-}$: 40 ± 4%, n = 5), proximal colon (WT: 34 ± 7%, n = 5; Nlgn3$^{-/-}$: 36 ± 11, n = 4), mid colon (WT: 24 ± 3%, n = 5; Nlgn3$^{-/-}$: 21 ± 3%, n = 8), and distal colon (WT: 32 ± 6%, n = 6; Nlgn3$^{-/-}$: 32 ± 4%, n = 7) in WT and Nlgn3$^{-/-}$ mice (P = 0.67, two-way ANOVA, Fig. 2).

Neuroligin-3 protein expression was assessed using immunoprecipitation and Western blot in brain, proximal colon, and distal colon of WT and Nlgn3$^{-/-}$ tissue (Fig. 3). Neuroligin-3 migrated at approximately 100 kDa in WT tissue as previously reported [Varoqueaux et al., 2006]. This band was absent in all Nlgn3$^{-/-}$-derived samples.

To determine if NL3 deletion affects gut diameter and contractility in the absence of input from the central nervous system, we undertook *ex vivo* video imaging analysis of colon diameter and spontaneous CMMCs as previously reported [Swaminathan et al., 2016] in WT and Nlgn3$^{-/-}$ mice. Nlgn3$^{-/-}$ mice had increased resting colonic diameters compared to WT mice under control conditions (WT: 3.4 ± 0.2 mm, n = 16; Nlgn3$^{-/-}$: 4.0 ± 0.1 mm, n = 15, P = 0.03,

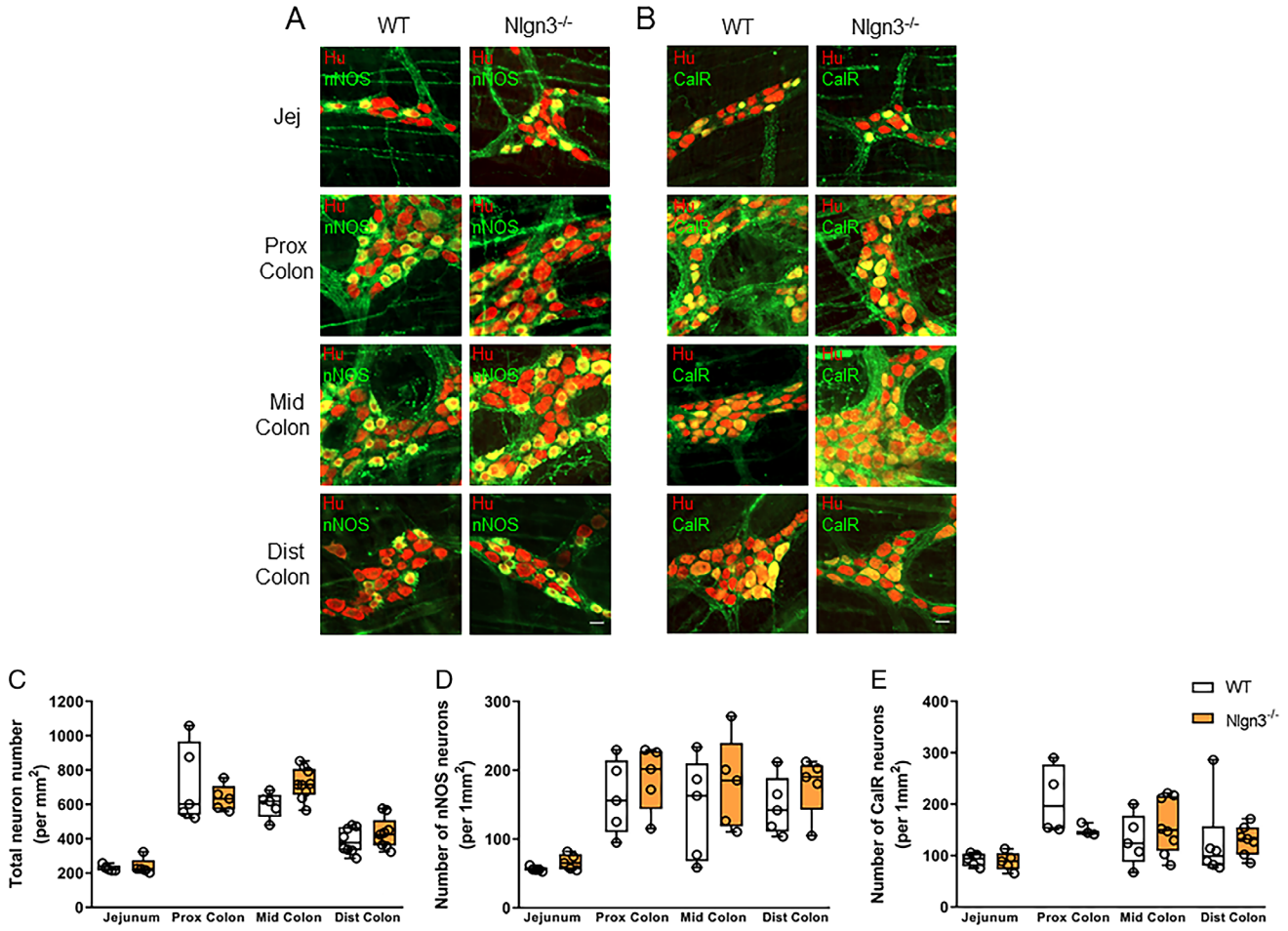

Figure 2. Numbers of myenteric neurons expressing nNOS and CalR in WT and Nlgn3$^{-/-}$ mice. (**A**) Neurons expressing neuronal nitric oxide synthase (nNOS; green) and Hu (red) in the jejunum, proximal colon, mid colon, and distal colon, with colocalization evident in yellow. (**B**) Neurons expressing calretinin (CalR; green) and Hu (red), with colocalization evident in yellow. (**C**) Mean number of neurons expressing Hu per mm^2. (**D**) Number of neurons expressing nNOS. (**E**) Number of neurons expressing CalR. Scale bar: 20 μm. Statistics: two-way ANOVA.

Fig. 4A–C). However, there was no significant difference in the number of CMMCs between WT and Nlgn3$^{-/-}$ mice (WT: 8.4 ± 1 CMMCs/15 min, n = 19; Nlgn3$^{-/-}$: 9.4 ± 1 CMMCs/15 min, n = 16, P = 0.34, Fig. 4D). Interestingly, Nlgn3$^{-/-}$mice showed significantly faster CMMC speeds compared to WT mice (WT: 1.8 ± 0.1 mm/s, n = 15; Nlgn3$^{-/-}$: 2.4 ± 0.2 mm/s, n = 17, P = 0.04, Fig. 4A, B, and E).

To assay for differential effects of NO in WT and Nlgn3$^{-/-}$ mice, resting colon diameter and number and speed of CMMCs were assessed in the presence of NOLA, an inhibitor of nitric oxide synthase (NOS). It is well established that NOLA increases CMMC frequency [Powell & Bywater, 2001; Roberts et al., 2007]. To determine the magnitude of the effect of NOLA on the colon, we calculated the percentage change in motility parameters between NOLA and baseline conditions. In the presence of NOLA, both Nlgn3$^{-/-}$ and WT mice showed a similar percentage decrease in gut width compared to baseline (WT: 23 ± 3%, n = 16; Nlgn3$^{-/-}$: 20 ± 4%, n = 14, P = 0.52, Fig. 5A–C; raw values: WT: 2.6 ± 0.2 mm, n = 15; Nlgn3$^{-/-}$: 3.2 ± 0.2 mm, n = 18). CMMC frequency in NOLA was also similar in WT and Nlgn3$^{-/-}$ mice (WT: 32 ± 12% CMMCs/15 min, n = 18; Nlgn3$^{-/-}$: 41 ± 15% CMMCs/15 min, n = 15, P = 0.64, Fig. 5D; raw values: WT: 10.1 ± 0.5 CMMCs/15 min, n = 15; Nlgn3$^{-/-}$: 11.6 ± 0.7 CMMCs/15 min, n = 18). However, Nlgn3$^{-/-}$ mice showed reduced sensitivity to NOLA as demonstrated by a smaller increase in CMMC speed in the presence of NOLA compared to WT mice (WT: 136 ± 27% mm/s, n = 15; Nlgn3$^{-/-}$: 54 ± 20% mm/s, n = 18, P = 0.02, Fig. 5E; raw values: WT: 3.92 ± 0.24 mm/s, n = 15; Nlgn3$^{-/-}$: 3.36 ± 0.29 mm/s, n = 18).

Discussion

This study aimed to determine the role of the synaptic adhesion molecule Neuroligin-3 in the structure and function of the GI tract by analyzing mucosal epithelial structure, the

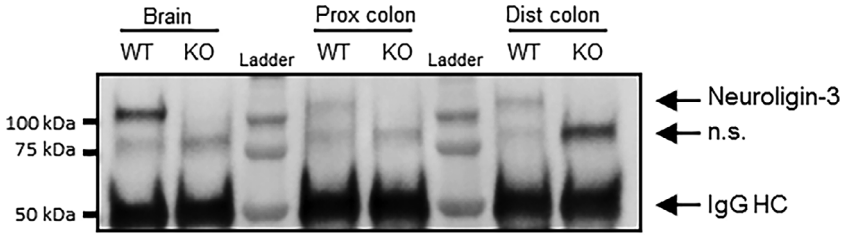

Figure 3. Confirmation of Neuroligin-3 expression in colon tissue. Neuroligin-3 protein expression is present in colon and brain of WT but absent in Nlgn3$^{-/-}$ (KO) mice. Neuroligin-3 was immunoprecipitated from the brain, proximal colon, and distal colon of a WT mouse and a Nlgn3$^{-/-}$ mouse, and subjected to SDS-PAGE and Western immunoblotting with an antibody to Neuroligin-3. n.s., non-specific band; IgG HC, IgG heavy chain.

neurochemistry of myenteric neurons and colonic motility in the Nlgn3$^{-/-}$ mouse model of autism. We reveal that Nlgn3$^{-/-}$ mice have similar mucosal structure in the small and large intestine, and no change in myenteric neuronal numbers in the proximal jejunum or colon compared to WT mice. Nlgn3$^{-/-}$ mice show both decreased colonic smooth muscle tone and altered colonic motility. Specifically, Nlgn3$^{-/-}$ mice have an increased colonic diameter and faster CMMCs under baseline conditions. In the presence of the nNOS inhibitor NOLA, Nlgn3$^{-/-}$ mice showed a smaller increase in CMMCs compared to WT mice.

Changes in GI tract mucosal morphology are reported in both the clinical setting and in animal models of autism, therefore we assessed for similar changes in Nlgn3$^{-/-}$ mice. For example, partial villus atrophy [Horvath et al., 1999], cryptitis, and crypt branching [Krigsman et al., 2010] have been documented in patients with autism. Mice with modified serotonin reuptake transporter (SERT) function due to the autism-associated rare coding variant Ala56 (G56A) showed reduced villus height and crypt depth [Margolis et al., 2016]. Mice lacking SERT (SERT KO) showed increased villus height and crypt depth. In contrast, with these findings in the clinic and in other animal models of autism, Nlgn3$^{-/-}$ mice jejunal and colon villus height and crypt depth were unaltered suggesting that *Nlgn3* deletion does not overtly disrupt development and maintenance of the mucosal epithelium.

We observed similar neuronal numbers in the proximal jejunum and proximal, mid and distal colon of Nlgn3$^{-/-}$ mice, suggesting that Nlgn3$^{-/-}$ mice do not exhibit a major morphological phenotype in the MP of these regions of the GI tract. In contrast, myenteric neurons are decreased in the colon of SERT G56A mice, whereas SERT KO mice showed increased numbers of colonic myenteric neurons [Margolis et al., 2016]. There were also no changes in the number of cells immunofluorescent for the two neuronal markers examined (i.e., NOS and CalR). Although neither the overall number of neurons nor the numbers of two subtypes of neurons were altered, the *Nlgn3* deletion may potentially impact GI function via modifying synaptic (i.e., varicosity) densities. Further work using high-resolution microscopy techniques to assess for such changes is required in these mice.

Here we show evidence for a subtle GI dysfunction phenotype in Nlgn3$^{-/-}$ mouse colon. Using an *ex vivo* assay for motility enables ENS function to be assessed in the absence of input from the brain. We propose that the deletion of *Nlgn3* reduced colonic smooth muscle tone leading to an increased resting colonic diameter, likely due to altered innervation of the smooth muscle. Other biological mechanisms potentially underlying this change in diameter could involve a change in the function of interstitial cells of Cajal that are involved in regulating the "pacemaker" activity of enteric myenteric neurons. Alternatively, differences in the levels of NO production could be present despite our observation that nNOS cell numbers are unchanged. Neuronal NO is a prominent inhibitory neurotransmitter synthesized by myenteric inhibitory motor neurons and interneurons [Sang & Young, 1996] that regulates smooth muscle relaxation between CMMCs [Brookes, 1993, Spencer, 2001]. Interestingly, under baseline conditions Nlgn3$^{-/-}$ mice showed significantly faster CMMCs compared to WT colons. Although NOLA further increased CMMC speed in both genotypes, unsurprisingly, we observed a larger percentage change in WT than in Nlgn3$^{-/-}$ mice given that WT had slower CMMCs at baseline. In light of our findings indicating no change in nNOS+ neuron numbers, the increased CMMC speed in Nlgn3$^{-/-}$ mice could be due to altered expression of nNOS in circular smooth muscle cells [Grider et al., 1992], aberrant innervation of GI smooth muscle by nNOS neurons, or increased numbers of nNOS+ varicosities, which may cause an increase in NO in the ENS. The persistence of this fast CMMC phenotype in the presence of the NOS inhibitor NOLA suggests that it is not solely due to NO-mediated relaxation. There have been important advances in the understanding of the neuronal mechanisms underlying CMMCs in mice, such that each event involves coordinated neuronal firing of large populations of myenteric neurons [Spencer et al., 2018; Spencer, Dinning, Brookes, & Costa, 2016]. Although the numbers of myenteric neurons were not overtly different between the WT and Nlgn$^{-/-}$ mice, it is possible that there are differences in synaptic activation of the interneurons that underlie CMMC generation, which could contribute to the differences detected.

The subtle nature of the GI tract changes in Nlgn3$^{-/-}$ mice could be due to compensatory mechanisms occurring at

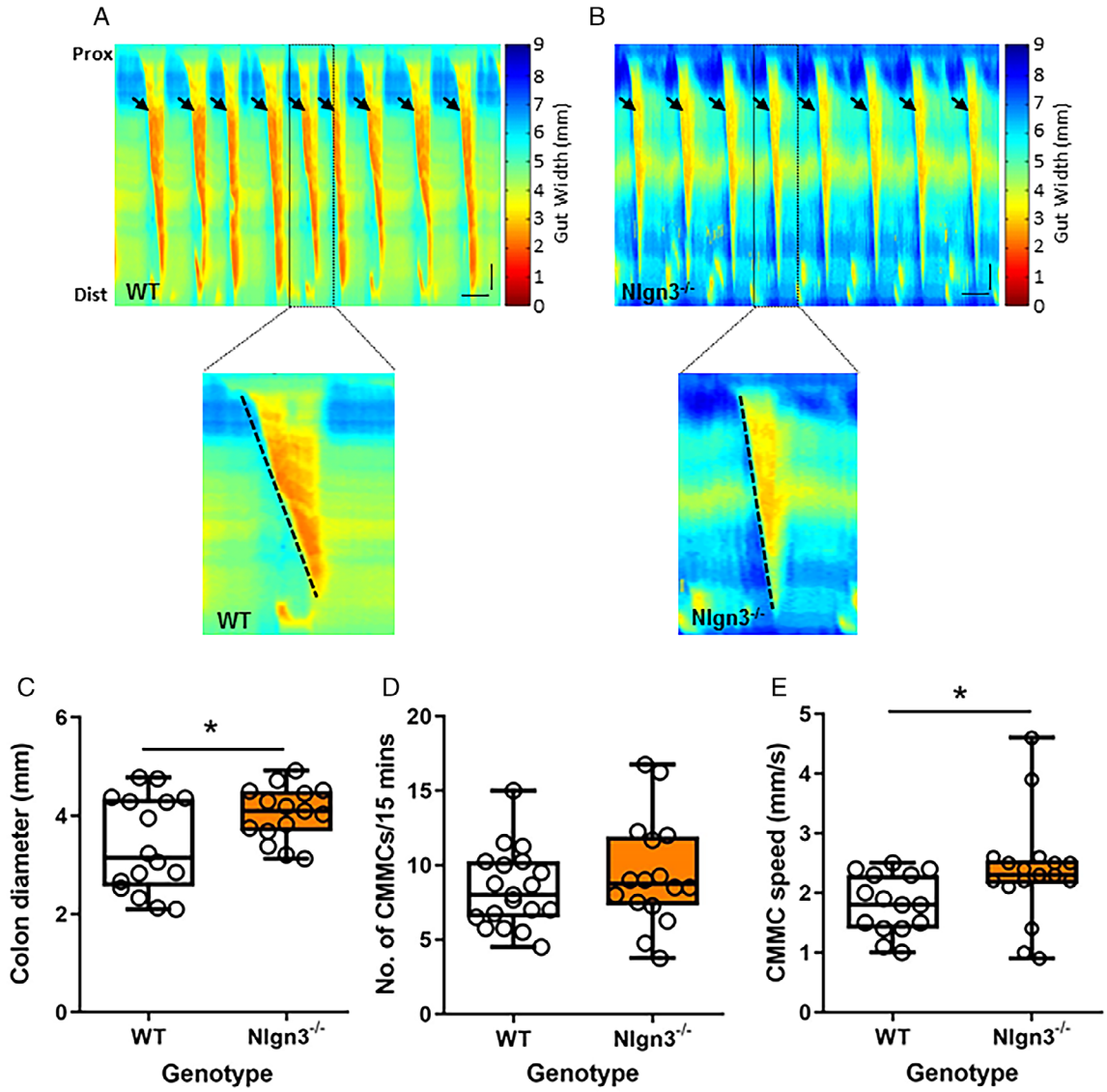

Figure 4. Baseline measurements of resting colon diameter and numbers of colonic migrating motor complexes (CMMCs) between WT and Nlgn3$^{-/-}$ mice. (**A**, **B**) Spatiotemporal maps showing baseline CMMCs in WT (**A**) and Nlgn3$^{-/-}$ (**B**) mice. (**C**) Resting gut diameter was higher in Nlgn3$^{-/-}$ mice (n = 16) compared to WT mice (n = 15, P = 0.03). (**D**) No difference in the number of CMMCs/15 min was observed between WT mice (n = 16) and Nlgn3$^{-/-}$ (n = 19, P = 0.38). (**E**) Nlgn3$^{-/-}$mice (n = 17) had increased speed of CMMCs compared to WT mice (n = 15, P = 0.04). Statistics: Student's t test, Bonferroni post hoc test, Number of CMMCs assessed via Mann–Whitney test, *P < 0.05. Horizontal scale bar = Time (1 min). Vertical scale bar = 0.5 cm (length of colon). The color scale on the right of each map indicates the width of the gut for each captured frame during the 15-min recording. Arrows indicate individual CMMCs. The broken lines within the enlarged regions of the spatiotemporal maps in A and B highlight the gradient (speed) of the CMMCs.

the synaptic level. Neuroligin-3 forms heterodimers with Neuroligin-1 [Poulopoulos et al., 2012], which is found exclusively at excitatory synapses in the brain [Levinson et al., 2005]. Nlgn3$^{-/-}$ mice show decreased Neuroligin-1 levels in the forebrain [Tabuchi et al., 2007]; additionally, Nlgn1/Nlgn3 double knockout mice have a more severe phenotype compared to Nlgn3$^{-/-}$ mice [Varoqueaux et al., 2006]. *Nlgn3* may play much larger roles in CMMC properties than detected in the current study if *Nlgn3* was acutely obliterated using an inducible genetic deletion model, rather than double constitutive knockouts from birth (due to the compensatory mechanisms occurring in the physiological environment in knockouts from birth). However, the current constitutive deletion model is relevant for clinical studies where the gene deletion is present throughout life. The background strain of these mice may also influence the severity of the GI phenotype as has been shown for other models expressing autism-associated mutations in Nlgn3 [Jaramillo et al., 2018]. Additional studies investigating potential changes to the GI tract of Nlgn1/Nlgn3 double knockout mice, as well as Nlgn1$^{-/-}$ mice on different background strains, would allow a more comprehensive understanding

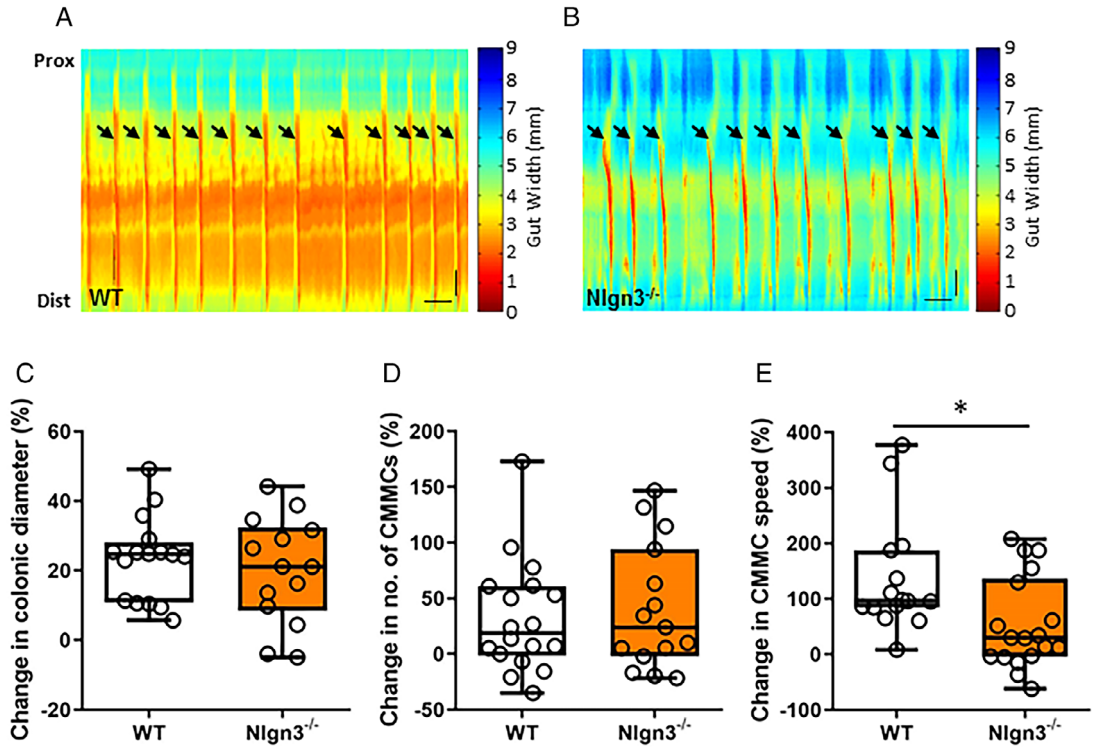

Figure 5. Change in colonic parameters in WT and Nlgn3$^{-/-}$ mice in the presence of NOLA. (**A**, **B**) Spatiotemporal maps showing CMMCs in the presence of NOLA in WT (**A**) and Nlgn3$^{-/-}$ (**B**) mice. (**C**) Percentage change in resting gut diameter was similar in Nlgn3$^{-/-}$ mice (n = 14) and WT mice (n = 16, P = 0.52). (**D**) No difference in percentage change of the number of CMMCs/15 min was observed between WT mice (n = 18) and Nlgn3$^{-/-}$ (n = 15, P = 0.64). (**E**) Nlgn3$^{-/-}$mice (n = 18) showed a smaller increase in CMMC speed compared to WT mice (n = 15, P = 0.02) once NOLA was added to the organ bath. Statistics: Student's t test, Bonferroni post hoc test, *P < 0.05. Horizontal scale bar = 1 min. Vertical scale bar = 0.5 cm (length of colon). The color scale on the right of each map indicates the width of the gut for each capture frame during the 15-min recording. Arrows indicate individual CMMCs.

of the roles of Neurolign-1 and Neuroligin-3 in GI structure and function.

Our findings support an emerging theme of altered GI function in genetic models of autism that has relevance for understanding GI dysfunction in individuals with neurodevelopmental disorders. A recent study of SERT G56A mice revealed both functional changes as well as decreased numbers of neurons in the MP, and decreased villus height and crypt depth in the GI tract [Margolis et al., 2016]. SERT G56A mice also exhibited decreased colonic motility [Margolis et al., 2016]. Other models of autism including mice and zebrafish heterozygous for the chromatin-remodeling gene CHD8 also display altered GI function in addition to changes in anatomical structure and neuronal numbers [Bernier et al., 2014; Katayama et al., 2016]. Emerging evidence that autism-associated mutations impact the ENS provides opportunities for application of extracerebral functional assays and preclinical therapy design in animal models. In summary, our findings indicate that an autism-associated mutation in Neuroligin-3 results in GI dysfunction and highlights a need for detailed characterization of ENS function in animal models of autism.

Acknowledgments

This work was supported by Australian Research Council Future Fellowship (FT160100126) to E.L.H.-Y. and National Health and Medical Research Council Project Grant (APP1083334) and Australian Research Council Future Fellowship (FT140101327) to J.N. E.L.H.-Y. also received an RMIT Vice Chancellor's Senior Research Fellowship, which supported G.K.B. The Hu antibody was a gift from Dr. V. Lennon, Mayo Clinic, USA.

Conflict of Interest

The authors declare that there is no conflict of interest.

References

Alarcón, M., Abrahams, B. S., Stone, J. L., Duvall, J. A., Perederiy, J. V., Bomar, J. M., … Nelson, S. F. (2008). Linkage, association, and gene-expression analyses identify CNTNAP2 as an autism-susceptibility gene. The American Journal of Human Genetics, 82(1), 150–159.

American Psychiatric Association. (2013). Diagnostic and statistical manual of mental disorders (DSM-5®). Washington, DC: American Psychiatric Association.

Arking, D. E., Cutler, D. J., Brune, C. W., Teslovich, T. M., West, K., Ikeda, M., … Chakravarti, A. (2008). A common genetic variant in the neurexin superfamily member CNTNAP2 increases familial risk of autism. The American Journal of Human Genetics, 82 (1), 160–164.

Bailey, A., Le Couteur, A., Gottesman, I., Bolton, P., Simonoff, E., Yuzda, E., & Rutter, M. (1995). Autism as a strongly genetic disorder: Evidence from a British twin study. Psychological Medicine, 25, 63–77.

Baio, J., Wiggins, L., Christensen, D. L., Maenner, M. J., Daniels, J., Warren, Z., … Dowling, N. F. (2018). Prevalence of autism spectrum disorder among children aged 8 years—Autism and developmental disabilities monitoring network, 11 sites, United States, 2014. MMWR Surveillance Summary, 67(SS-6), 1–23. https://doi.org/10.15585/mmwr.ss6706a1.

Bakkaloglu, B., O'Roak, B. J., Louvi, A., Gupta, A. R., Abelson, J. F., Morgan, T. M., … Tanriover, G. (2008). Molecular cytogenetic analysis and resequencing of contact in associated protein-like 2 in autism spectrum disorders. The American Journal of Human Genetics, 82(1), 165–173.

Balasuriya, G. K., Hill-Yardin, E. L., Gershon, M. D., & Bornstein, J. C. (2016). A sexually dimorphic effect of cholera toxin: rapid changes in colonic motility mediated via a 5-HT3 receptor-dependent pathway in female C57Bl/6 mice. The Journal of Physiology, 594, 4325–4338.

Basu, S. N., Kollu, R., & Banerjee-Basu, S. (2009). AutDB: A gene reference resource for autism research. Nucleic Acids Research, 37 (suppl_1), D832–D836.

Bernier, R., Golzio, C., Xiong, B., Stessman, H. A., Coe, B. P., Penn, O., … Eichler, E. E. (2014). Disruptive CHD8 mutations define a subtype of autism early in development. Cell, 158(2), 263–276.

Bertrand, P. P., Kunze, W. A. A., Bornstein, J. C., Furness, J. B., & Smith, M. L. (1997). Analysis of the responses of myenteric neurons in the small intestine to chemical stimulation of the mucosa. American Journal of Physiology - Gastrointestinal and Liver Physiology, 273, G422–G435.

Betancur, C. (2011). Etiological heterogeneity in autism spectrum disorders: More than 100 genetic and genomic disorders and still counting. Brain Research, 1380, 42–77.

Betancur, C., Sakurai, T., & Buxbaum, J. D. (2009). The emerging role of synaptic cell-adhesion pathways in the pathogenesis of autism spectrum disorders. Trends in Neurosciences, 32(7), 402–412.

Bourgeron, T. (2009). A synaptic trek to autism. Current Opinion in Neurobiology, 19(2), 231–234.

Bourgeron, T. (2015). From the genetic architecture to synaptic plasticity in autism spectrum disorder. Nature Reviews Neuroscience, 16(9), 551–563.

Brookes, S. J. (1993). Neuronal nitric oxide in the gut. Journal of Gastroenterology and Hepatology, 8, 590–603.

Brookes, S. J. (2001). Classes of enteric nerve cells in the Guinea pig small intestine. The Anatomical Record, 262, 58–70.

Comoletti, D., De Jaco, A., Jennings, L. L., Flynn, R. E., Gaietta, G., Tsigelny, I., … Taylor, P. (2004). The Arg451Cys-neuroligin-3 mutation associated with autism reveals a defect in protein processing. The Journal of Neuroscience, 24, 4889–4893.

Cristino, A. S., Williams, S. M., Hawi, Z., An, J. Y., Bellgrove, M. A., Schwartz, C. E., … Claudianos, C. (2014). Neurodevelopmental and neuropsychiatric disorders represent an interconnected molecular system. Molecular Psychiatry, 19, 294–301.

Croen, L. A., Najjar, D. V., Ray, G. T., Lotspeich, L., & Bernal, P. (2006). A comparison of health care utilization and costs of children with and without autism spectrum disorders in a large group-model health plan. Pediatrics, 118, e1203–e1211.

Durand, C. M., Betancur, C., Boeckers, T. M., Bockmann, J., Chaste, P., Fauchereau, F., … Bourgeron, T. (2007). Mutations in the gene encoding the synaptic scaffolding protein Shank3 are associated with autism spectrum disorders. Nature Genetics, 39, 25–27.

Etherton, M., Földy, C., Sharma, M., Tabuchi, K., Liu, X., Shamloo, M., … Südhof, T. C. (2011). Autism-linked neuroligin-3 R451C mutation differentially alters hippocampal and cortical synaptic function. Proceedings of the National Academy of Sciences, 108, 13764–13769.

Feyder, M., Karlsson, R. M., Mathur, P., Lyman, M., Bock, R., Momenan, R., … Graybeal, C. (2010). Association of mouse Dlg4 (PSD-95) gene deletion and human DLG4 gene variation with phenotypes relevant to autism spectrum disorders and Williams' syndrome. American Journal of Psychiatry, 167(12), 1508–1517.

Földy, C., Malenka, R. C., & Südhof, T. C. (2013). Autism-associated neuroligin-3 mutations commonly disrupt tonic endocannabinoid signalling. Neuron, 78, 498–509.

Folstein, S. E., & Rosen-Sheidley, B. (2001). Genetics of autism: Complex aetiology for a heterogenous disorder. Nature Reviews Genetics, 2, 943–955.

Furness, J. B. (2000). Types of neurons in the entericnervous system. Journal of the Autonomic Nervous System, 81(1-3), 87–96.

Furness, J. B. (2006). The enteric nervous system. Victoria, Australia: Blackwell Publishing.

Furness, J. B. (2012). The enteric nervous system and neurogastroenterology. Nature Reviews Gastroenterology & Hepatology, 9(5), 286–294.

Geschwind, D. H. (2011). Genetics of autism spectrum disorders. Trends in Cognitive Sciences, 15, 409–416.

Grider, J. R., Murthy, K. S., Jin, J. G., & Makhlouf, G. M. (1992). Stimulation of nitric oxide from muscle cells by VIP: prejunctional enhancement of VIP release. American Journal of Physiology-Gastrointestinal and Liver Physiology, 262(4), G774–G778.

Holingue, C., Newill, C., Lee, L. C., Pasricha, P. J., & Daniele Fallin, M. (2018). Gastrointestinal symptoms in autism spectrumdisorder: A review of the literature on ascertainment and prevalence. Autism Research, 11(1), 24–36.

Horvath, K., Papadimitriou, J. C., Rabsztyn, A., Drachenberg, C., & Tildon, J. T. (1999). Gastrointestinal abnormalities in children with autistic disorder. The Journal of Pediatrics, 135, 559–563.

Jamain, S., Quach, H., Betancur, C., Råstam, M., Colineaux, C., Gillberg, I. C., … Gillberg, C. (2003). Mutations of the X-linked genes encoding neuroligins NL3 and NLGN4 are associated with autism. Nature Genetics, 34, 27–29.

Jaramillo, T. C., Escamilla, C. O., Liu, S., Peca, L., Birnbaum, S. G., & Powell, C. M. (2018). Genetic background effects in Neuroligin-3 mutant mice: Minimal behavioral abnormalities on C57 background. Autism Research, 11(2), 234–244.

Jaramillo, T. C., Liu, S., Pettersen, A., Birnbaum, S. G., & Powell, C. M. (2014). Autism-related neuroligin-3 mutation alters social behavior and spatial learning. Autism Research, 7(2), 264–272.

Katayama, Y., Nishiyama, M., Shoji, H., Ohkawa, Y., Kawamura, A., Sato, T., … Nakayama, K. I. (2016). CHD8 haploinsufficiency results in autistic-like phenotypes in mice. Nature, 537(7622), 675–679.

Krigsman, A., Boris, M., Goldblatt, A., & Stott, C. (2010). Clinical presentation and histologic findings at ileocolonoscopy in childrenwith autistic spectrum disorder and chronic gastrointestinal symptoms. Autism Insights, 2010(2), 1–11.

Levinson, J. N., Chéry, N., Huang, K., Wong, T. P., Gerrow, K., Kang, R., … El-Husseini, A. (2005). Neuroligins mediate excitatory and inhibitory synapse formation: Involvement of PSD95 and neurexin-1β in neuroligin-induced synaptic specificity. Journal of Biological Chemistry, 280(17), 17312–17319.

Levy, D., Ronemus, M., Yamrom, B., Lee, Y. H., Leotta, A., Kendall, J., … Buja, A. (2011). Rare de novo and transmitted copy-number variation in autistic spectrum disorders. Neuron, 70(5), 886–897.

Margolis, K. G., Li, Z., Stevanovic, K., Saurman, V., Israelyan, N., Anderson, G. M., … Gershon, M. D. (2016). Serotonin transporter variant drives preventable gastrointestinal abnormalities in development and function. The Journal of Clinical Investigation, 126, 2221–2235.

McElhanon, B. O., Mccracken, C., Karpen, S., & Sharp, W. G. (2014). Gastrointestinal symptoms in autism spectrum disorder: A meta-analysis. Pediatrics, 133, 872–883.

Moessner, R., Marshall, C. R., Sutcliffe, J. S., Skaug, J., Pinto, D., Vincent, J., … Scherer, S. W. (2007). Contribution of Shank3 mutations to autism spectrum disorder. American Journal of Human Genetics, 81, 1289–1297.

Phelan, M. C., Rogers, R. C., Saul, R. A., Stapleton, G. A., Sweet, K., Mcdermid, H., … Kelly, D. P. (2001). 22q13 deletion syndrome. American Journal of Medical Genetics, 101, 91–99.

Poulopoulos, A., Soykan, T., Tuffy, L. P., Hammer, M., Varoqueaux, F., & Brose, N. (2012). Homodimerization and isoform-specific heterodimerization of neuroligins. Biochemical Journal, 446(2), 321–330.

Powell, A. K., & Bywater, R. A. R. (2001). Endogenousnitric oxide release modulates the direction and frequency of colonic migratingmotor complexes in the isolated mouse colon. Neurogastroenterology & Motility, 13(3), 221–228.

Radyushkin, K., Hammerschmidt, K., Boretius, S., Varoqueaux, F., El-Kordi, A., Ronnenberg, A., … Brose, N. (2009). Neuroligin-3-deficient mice: Model of a monogenic heritable form of autism with an olfactory deficit. Genes, Brain and Behavior, 8, 416–425.

Roberts, R. R., Murphy, J. F., Young, H. M., & Bornstein, J. C. (2007). Development of colonic motility in the neonatalmouse-studies using spatiotemporal maps. American Journal of Physiology-Gastrointestinal and Liver Physiology, 292(3), G930–G938.

Sanders, S. J., Ercan-Sencicek, A. G., Hus, V., Luo, R., Murtha, M. T., Moreno-De-Luca, D., … Mason, C. E. (2011). Multiple recurrent de novo CNVs, including duplications of the 7q11. 23 Williams syndrome region, are strongly associated with autism. Neuron, 70(5), 863–885.

Sang, Q., & Young, H. M. (1996). Chemical coding of neurons in the myenteric plexus and external muscle of the small and large intestine of the mouse. Cell and Tissue Research, 284, 39–53.

Shen, C., Huo, L.-R., Zhao, X.-L., Wang, P.-R., & Zhong, N. (2015). Novel interactive partners of neuroligin 3: New aspects for pathogenesis of autism. Journal of Molecular Neuroscience, 56, 89–101.

Spencer, N. J. (2001). Control of migrating motor activity inthe colon. Current Opinion in Pharmacology, 1(6), 604–610.

Spencer, N. J., Dinning, P. G., Brookes, S. J., & Costa, M. (2016). Insights into the mechanisms underlying colonic motor patterns. Journal of Physiology, 594(15), 4099–4116.

Spencer, N. J., Hibberd, T. J., Travis, L., Wiklendt, L., Costa, M., Hu, H., … Sorensen, J. (2018). Identification of a rhythmic firing pattern in the enteric nervous system that generates rhythmic electrical activity in smooth muscle. The Journal of Neuroscience, 38(24), 5507–5522.

Steffenburg, S., Gillberg, C., Hellgren, L., Andersson, L., Gillberg, C., Jakobsson, G., & Bohman, M. (1989). A twin study of autism in Denmark, Finland, Iceland, Norway and Sweden. Journal of Child Psychology and Psychiatry, 30, 405–416.

Sudhof, T. C. (2008). Neuroligins and neurexins link synaptic function to cognitive disease. Nature, 455, 903–911.

Surawicz, C. M. (2010). Mechanisms of diarrhea. Current Gastroenterology Reports, 12, 236–241.

Swaminathan, M., Hill-Yardin, E., Ellis, M., Zygorodimos, M., Johnston, L. A., Gwynne, R. M., & Bornstein, J. C. (2016). Video imaging and spatiotemporal maps to analyze gastrointestinal motility in mice. Journal of Visualized Experiments, 108, 53828.

Tabuchi, K., Blundell, J., Etherton, M. R., Hammer, R. E., Liu, X., Powell, C. M., & Sudhof, T. C. (2007). A neuroligin-3 mutation implicated in autism increases inhibitory synaptic transmission in mice. Science, 318, 71–76.

Valicenti-Mcdermott, M., Mcvicar, K., Rapin, I., Wershil, B. K., Cohen, H., & Shinnar, S. (2006). Frequency of gastrointestinal symptoms in children with autistic spectrum disorders and association with family history of autoimmune disease. Journal of Developmental & Behavioral Pediatrics, 27, S128–S136.

Varoqueaux, F., Aramuni, G., Rawson, R. L., Mohrmann, R., Missler, M., Gottmann, K., … Brose, N. (2006). Neuroligins determine synapse maturation and function. Neuron, 51, 741–754.

Voineagu, I., Wang, X., Johnston, P., Lowe, J. K., Tian, Y., Horvath, S., … Geschwind, D. H. (2011). Transcriptomic analysis of autistic brain reveals convergent molecular pathology. Nature, 474, 380–384.